Inorg. Chem. **2002**, *41*, 3761–3768

New Tetrathiapentalene-Derived Charge Transfer Salts with Paramagnetic Transition Metal Complex Anion: κ-(EDDH-TTP)$_3$[Cr(phen)(NCS)$_4$]·2CH$_2$Cl$_2$ and κ_{21}-(BDH-TTP)$_5$[Cr(phen)(NCS)$_4$]$_2$·2CH$_2$Cl$_2$

Fatima Setifi,[†] Lahcène Ouahab,*[,†] Stéphane Golhen,[†] Olivier Hernandez,[†] Akira Miyazaki,[‡] Toshiaki Enoki,[‡] Takashi Toita,[§] Jun-ichi Yamada,[§] Hiroyuki Nishikawa,[||] Andrzej Łapiński,[⊥] and Roman Świetlik[⊥]

Laboratoire de Chimie du Solide et Inorganique Moléculaire, UMR 6511 CNRS, Université de Rennes 1, Institut de Chimie de Rennes, 35042 Rennes Cedex, France, Department of Chemistry, Graduate School of Science and Engineering, Tokyo Institute of Technology, 2-12-1 Ookayama, Meguro-ku, Tokyo 152-8551, Japan, Department of Material Science, Faculty of Science, Himeji Institute of Technology, 3-2-1 Kouto, Kamigori-cho Ako-gun, Hyogo 678-1297, Japan, Department of Chemistry, Graduate School of Science, Tokyo Metropolitan University, 1-1 Minami-Ohsawa, Hachioji, Tokyo 192-0397, Japan, and Institute of Molecular Physics, Polish Academy of Sciences, Smoluchowskiego 17, 60-179 Poznań, Poland

Received March 14, 2002

The preparation, crystal structures, and optical and magnetic properties of two new charge-transfer salts κ-(EDDH-TTP)$_3$[Cr(phen)(NCS)$_4$]·2CH$_2$Cl$_2$ (**1**) and κ_{21}-(BDH-TTP)$_5$[Cr(phen)(NCS)$_4$]$_2$·2CH$_2$Cl$_2$ (**2**), where phen = 1,10-phenanthroline, EDDH-TTP = 2-(4,5-ethylenedithio-1,3-dithiol-2-ylidene)-5-(1,3-dithiolan-2-ylidene)-1,3,4,6-tetrathiapentalene, and BDH-TTP = 2,5-bis(1,3-dithiolan-2-ylidene)-1,3,4,6-tetrathiapentalene, are reported. Crystal data: (**1**) monoclinic $P2_1/a$, a = 25.0752(5) Å, b = 10.6732(3) Å, c = 28.1601(6) Å, β = 95.195(2)°, Z = 4, R = 0.0585 for 6741 independent reflections with $I > 3\sigma(I)$; (**2**) monoclinic $P2_1/a$, a = 23.8275(4) Å, b = 9.1015 (2) Å, c = 27.0420(1) Å, β = 99.9297(8)°, Z = 4, R = 0.0530 for 4565 independent reflections with $I > 2\sigma(I)$. The crystal structures for both compounds consist of alternating organic and inorganic layers. The organic layer in compound **1** is characterized as κ-type, while the organic layer in **2** resembles the κ-type but it contains orthogonal dimers and monomers, and it is therefore called κ_{21}. Compound **1** shows metallic behavior down to low temperature. Salt **2** shows semiconductive behavior, which is explained as the result of either charge ordering owing to the κ_{21}-type structure or Peierls distortion due to the one-dimensional electronic nature. However, weak metallic behavior could be observed at 10 kbar above ca. 150 K and at 15 kbar above 170 K. The magnetic susceptibilities for both compounds show Curie–Weiss behavior, showing that the exchange interactions between the magnetic anions are weak. Polarized reflectance spectra of single crystals were measured over the spectral range from 650 to 7000 cm^{-1}. Moreover, absorption and diffusion reflectance spectra of powdered crystals dispersed in KBr (from 400 to 7000 cm^{-1}) were recorded. Vibrational and electronic features are discussed.

Introduction

Up to now, organic conducting and superconducting charge transfer (CT) salts, excluding fullerenes, were based on donors derived from tetrathiafulvalene (TTF) or acceptors derived from dmit (isotrithionedithiolate).[1] However, recently, new donor systems such as DHTTF (dihydrotetrathi-

* To whom correspondence should be addressed. E-mail: ouahab@univ-rennes1.fr.
[†] Université de Rennes 1.
[‡] Tokyo Institute of Technology.
[§] Himeji Institute of Technology.
[||] Tokyo Metropolitan University.
[⊥] Polish Academy of Sciences.

(1) (a) Williams, J. M.; Ferraro, J. R.; Thorn, R. J.; Carlson, K. D.; Geiser, U.; Wang, H.-H.; Kini, A. M.; Whangbo, M.-H. *Organic Superconductors. Synthesis, Structure, Properties and Theory*; Grimes, R. N., Ed.; Prentice Hall: Englewood Cliffs, NJ, 1992. (b) Ishiguro, T.; Yamaji, K.; Saito, G. *Organic Superconductors*; Springer-Verlag: Heidelberg, Germany, 1998.

10.1021/ic0255961 CCC: $22.00
Published on Web 06/13/2002

Chart 1

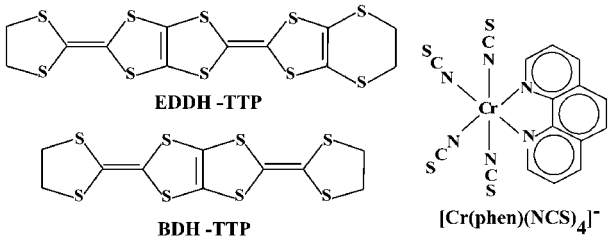

afulvalene)-TTF fused donors and tetrathiapentalene-based non-TTF donors have been developed.[2] For example, EDDH-TTP [2-(4,5-ethylenedithio-1,3-dithiol-2-ylidene)-5-(1,3-dithiolan-2-ylidene)-1,3,4,6-tetrathiapentalene][3] and BDH-TTP [2,5-bis(1,3-dithiolan-2-ylidene)-1,3,4,6-tetrathiapentalene][4] are found to produce κ-type metallic salts stable down to low temperatures (Chart 1). On the other hand, in the past few years, an increased interest was devoted to materials combining electrical conductivity and magnetic interactions, with the aim of obtaining magnetic coupling between the localized spins of the inorganic part (d-electrons) via the mobile electrons of the organic part (π-electrons).[5−15] Some compounds of this kind show a coexistence of superconductivity and paramagnetism as, for example, in (BEDT-TTF)$_4$[(H$_3$O)Fe(C$_2$O$_4$)$_3$]C$_6$H$_5$CN,[6b,c] (BEDT-TTF = bis(ethylenedithio)tetrathiafulvalene). In other cases, for example, (BEDT-TTF)$_3$[MnCr(C$_2$O$_4$)$_3$][11a] and (BO)$_3$[FeCr(C$_2$O$_4$)$_3$][11b] (BO = bis(ethylenedioxy)tetraselenafulvalene), the metallic state and ferromagnetism coexist. For most of these salts, however, the magnetic order is not mediated by the conducting electrons. Only within a few examples, such as, for instance, in λ-(BETS)$_2$FeCl$_4$ (BETS = bis(ethylenedithio)-tetraselenafulvalene)[7] and (DMET)$_2$FeBr$_4$ (DMET = dimethyl(ethylenedithio)diselenadithiafulvalene),[12] the π and d electrons play an important role in the magnetic interactions. To establish magnetic and/or structural interactions between the organic and inorganic sublattices, several strategies are under investigation. Using thiocyanato complexes [M^{III}(NCS)$_4$(L)$_n$]$^-$ where L = 1,10-phenanthroline (phen) or isoquinoline (isoq), which can enable both S···S and π···π interactions between the conducting and magnetic systems, Day's group obtained bulk ferrimagnetism in TTF-based salts with T_C's ranging from 4.2 to 8.9 K.[13] With the same anions combined with BDH-TTP donors, we obtained recently bulk weak ferromagnetism in (BDH-TTP)[M(NCS)$_4$-(isoq)$_2$], M = Cr^{III} and Fe^{III}, whose mechanism is discussed in detail on the basis of their crystal structure.[14] We report here the preparation, crystal structures, and optical and magnetic properties of κ-(EDDH-TTP)$_3$[Cr(phen)(NCS)$_4$]·2CH$_2$Cl$_2$ (**1**) and κ_{21}-(BDH-TTP)$_5$[Cr(phen)(NCS)$_4$]$_2$·2CH$_2$Cl$_2$ (**2**).

Experimental Section

Synthesis. All experiments were conducted under nitrogen or argon. The solvents were distilled before use, and the starting reagents were used as received. BDH-TTP,[2] EDDH-TTP,[16] and (Et$_4$N)[Cr(phen)(NCS)$_4$][13] were prepared following published methods. Black elongated plate crystals of compounds **1** and **2** were obtained on platinum wire electrodes (∅ = 1 mm) by galvanostatic oxidation (I = ca. 1.0 μA) of EDDH-TTP (10 mg) or BDH-TTF (10 mg), respectively, for **1** and **2**, using (Et$_4$N)[Cr(phen)(NCS)$_4$] (100 mg) in CH$_2$Cl$_2$ (20 mL) as a supporting electrolyte. The stoichiometries of target materials were checked by X-ray crystal structure analysis.

Crystallographic Data Collection and Structure Determination. Single crystals of the title compounds (**1** and **2**) were mounted on a Nonius four circle diffractometer equipped with a CCD camera and a graphite monochromated Mo Kα radiation source (λ = 0.71073 Å). Data collection was performed at 100 K for **1** and 120 K for **2**. Effective absorption correction was performed (SCALEPACK[17]). Structures were solved with SHELXS-97[18] and refined with CRYSTALS[19] by full matrix least-squares method on F for **1** and with SHELXL-97[18] programs by full matrix least-squares method on F^2 for **2**.

(2) Yamada, J.; Nishikawa, H.; Kikuchi, K. *J. Mater. Chem.* **1999**, *9*, 617.
(3) Yamada, J.; Mishima, S.; Anzai, H.; Tamura, M.; Nishio, Y.; Kajita, K.; Sato, T.; Nishikawa, H.; Ikemoto, I.; Kikuchi, K. *J. Chem. Soc., Chem. Commun*. **1996**, 2517.
(4) Yamada, J.; Watanabe, M.; Anzai, H.; Nishikawa, H.; Ikemoto, I.; Kikuchi, K. *Angew. Chem., Int. Ed*. **1999**, *38*, 810.
(5) (a) Henriques, R. T.; Alcacer, L.; Pouget, J. P.; Jérôme, D. *J. Phys. C: Solid State Phys.* **1984**, *17*, 5197. (b) Batail, P.; Ouahab, L.; Torrance, J. B.; Pylmann, M. L.; Parkin, S. S. P. *Solid State Commun.* **1985**, *55*−*7*, 597. (c) Anmuller, A.; Erk, P.; Klebs, G.; Hünig, S.; Schutz, J. U.; Werner, H. P. *Angew. Chem., Int. Ed. Engl.* **1986**, *25*, 740. (d) Ogawa, M. Y.; Martinsen, J.; Palmer, S. M.; Stanton, J. L.; Tanaka, J.; Greene, R. L.; Hoffman, B. M.; Ibers, J. A. *J. Am. Chem. Soc.* **1987**, *109*, 1115.
(6) (a) Day, P.; Kurmoo, M.; Mallah, T.; Marsden, I. R.; Friend, R. H.; Pratt, F. L.; Hayes, W.; Chasseau, D.; Gaultier, J.; Bravic, G.; Ducasse, L. *J. Am. Chem. Soc.* **1992**, *114*, 10722. (b) Graham, A. W.; Kurmoo, M.; Day, P. *J. Chem. Soc., Chem. Commun.* **1995**, 2061. (c) Turner, S. S.; Day, P.; Malik, K. M. A.; Hursthouse, M. B.; Teat, S. J.; MacLean, E. J.; Martin, L.; French, S. A. *Inorg. Chem.* **1999**, *38*, 3543.
(7) Kobayashi, H.; Kobayashi, A.; Cassoux, P. *Chem. Soc. Rev.* **2000**, *29*, 325 and references cited therein.
(8) (a) Le Maguerès, P.; Ouahab, L.; Conan, N.; Gomez-Garcìa, C. J.; Delhaès, P.; Even, J.; Bertault, M. *Solid State Commun.* **1996**, *97/1*, 27. (b) Le Maguerès, P.; Ouahab, L.; Briard, P.; Even, J.; Bertault, M.; Toupet, L.; Ramos, J.; Gomez-Garcìa, C. J.; Delhaès, P. *Mol. Cryst. Liq. Cryst.* **1997**, *305*, 479. (c) Gomez-Garcìa, C. J.; Ouahab, L.; Gimnenez-Saiz, C.; Triki, S.; Coronado, E.; Delhaès, P. *Angew. Chem., Int. Ed. Engl.* **1994**, *33-2*, 223.
(9) Enoki, T.; Yamaura, J.-I.; Miyazaki, A. *Bull. Chem. Soc. Jpn.* **1997**, *70*, 2005.
(10) Ouahab, L. *Chem. Mater.* **1997**, *9*, 1909.
(11) (a) Coronado, E.; Galan-Mascaros, J. R.; Gomez-Garcìa, C. J.; Laukhin, V. N. *Nature* **2000**, *408*, 447. (b) Yamochi, H.; Kawasaki, T.; Nagata, Y.; Maesato, M.; Saito, G. *Mol. Cryst. Liq. Cryst.* **2002**, *376*, 113.
(12) (a) Enomoto, K.; Miyazaki, A.; Enoki, T. *Synth. Met.* **2001**, *120*, 977. (b) Miyazaki, A.; Enomoto, M.; Enomoto, K.; Nishijo, J.; Enoki, T.; Ogura, E.; Kuwatani, Y.; Iyoda, M. *Mol. Cryst. Liq. Cryst.* **2002**, *376*, 535.
(13) (a) Turner, S. S.; Michaut, C.; Durot, S.; Day, D.; Gelbrich, T.; Hursthouse, M. B. *Dalton* **2000**, 905. (b) Turner, S. S.; Le Pevelen, D.; Day, D.; Prout, K. *Dalton* **2000**, 2739. (c) Setifi, F.; Golhen, S.; Ouahab, L.; Turner, S. S.; Day, P. *CrystEngComm* **2002**, *4*, 1.
(14) Setifi, F.; Golhen, S.; Ouahab, L.; Miyazaki, A.; Okabe, K.; Enoki, T.; Toita, T.; Yamada, J. *Inorg. Chem.*, in press.
(15) Yamada, J.; Toita, T.; Akutsu, H.; Nakatsuji, S.; Nishikawa, H.; Ikemoto, I.; Kikuchi, K. *J. Chem. Soc., Chem. Commun*. **2001**, 2538.
(16) Yamada, J.; Satoki, S.; Mishima, S.; Akashi, N.; Takahashi, K.; Masuda, N.; Nishimoto, Y.; Takasaki, S.; Anzai, H. *J. Org. Chem.* **1996**, *61*, 3987.
(17) Otwinowski, Z.; Minor, W. Processing of X-ray Diffraction Data Collected in Oscillation Mode. *Macromolecular Crystallography, part A*; Carter, C. W., Jr., Sweet, R. M., Eds.; Methods in Enzymology 276; Academic Press: New York, 1997; p 307−326.
(18) Sheldrick, G. M. *SHELX 97, Program for the Refinement of Crystal Structures*; University of Göttingen: Göttingen, Germany 1997.
(19) Watkin, D. J.; Prout, C. K.; Carruthers, J. R.; Betteridge, P. W. *CRYSTALS*; Chemical Crystallography Laboratory: Oxford, England 1999; issue 11.

For compound **1**, the asymmetric unit contains one $[Cr(phen)(NCS)_4]^-$ anion, three EDDH-TTP donor molecules (called **A**, **B**, and **C**), and two CH_2Cl_2 solvent molecules. These units belong to the general positions of the $P2_1/a$ monoclinic space group. Molecule **A** and the solvent molecules as well as the anion were refined anisotropically. Fourier difference syntheses reveal that each **B** and **C** molecule is split into two molecules (**B** and **B′** and **C** and **C′**) (see Figure 1a) that might be related to each other by a pseudo inversion center located at the center of gravity of the EDDH-TTP molecules. Because of the anisotropic shape of the donor molecule, these disorders should be ascribed to static ones rather than dynamical ones. Moreover, we did not detect any structural changes down to 100 K. The occupancy factors were found equal to 0.486(8) and 0.513(8) for **B** and **B′** and equal to 0.771(5) and 0.229(5) for **C** and **C′**. All the atoms belonging to the same molecule were refined with the same occupation factor. The four latter molecules have been refined individually by means of geometric (distance, angle, and planarity) soft restraints according to the molecular conformation of the ordered **A** molecule. For a given molecule, the isotropic displacement parameters of the sp^3 (sp^2) C atoms (of all the C atoms for the **C′** molecule) and of the S atoms related by the molecular inversion center were set to a single-least squares parameter, respectively.

Compound **2** crystallizes in the monoclinic space group $P2_1/a$. The asymmetric unit contains one anion in general position, three BDH-TTP molecules called **A**, **B**, and **C**; the **A** and **B** molecules are located on general position, while the **C** molecule is located at inversion center. The ORTEP diagram (see Figure 1b) shows that one terminal ethylenic carbon atom is disordered onto two sites each, C37a/C37b. Additionally, a disordered CH_2Cl_2 molecule can be found.

Crystallographic data are summarized in Table 1. Bond lengths and bond angles, atomic coordinates, and complete crystal structure results are given as Supporting Information.

Physical Property Measurements. Electrical conductivities were measured with the four-probe method down to 4.2 K, using gold wire (25 μm) and carbon paste to make contacts. The measurement under hydrostatic pressure was carried out using a clamped cell and Daphne 7373 oil (Idemitsu Co. Ltd.) as a pressure medium.[20] The value of the pressure quoted here corresponds to that of the clamped pressure at room temperature. Magnetic susceptibilities were measured using a Quantum Design MPMS-5 SQUID magnetometer with an applied field of 1 T for microcrystalline sample enclosed in an aluminum foil (**1**) or single crystalline sample (**2**).

The polarized reflectance spectra at nearly normal incidence were measured over the spectral range from 650 to 7000 cm^{-1} by using a Perkin-Elmer 1725X Fourier transform infrared (FTIR) spectrometer equipped with a Perkin-Elmer microscope and a gold-wire-grid polarizer. Additionally, we studied absorption and diffuse reflectance spectra of powdered crystals dispersed in KBr (from 400 to 7000 cm^{-1}).

Results and Discussion

Crystal Structures. Figure 1 shows ORTEP drawings of the molecular structures and the atom numbering scheme for both **1** and **2**.

***κ*-(EDDH-TTP)$_3$[Cr(phen)(NCS)$_4$]·2CH$_2$Cl$_2$ (1).** The mean values for Cr−N (NCS) distances and Cr−N (phenan-

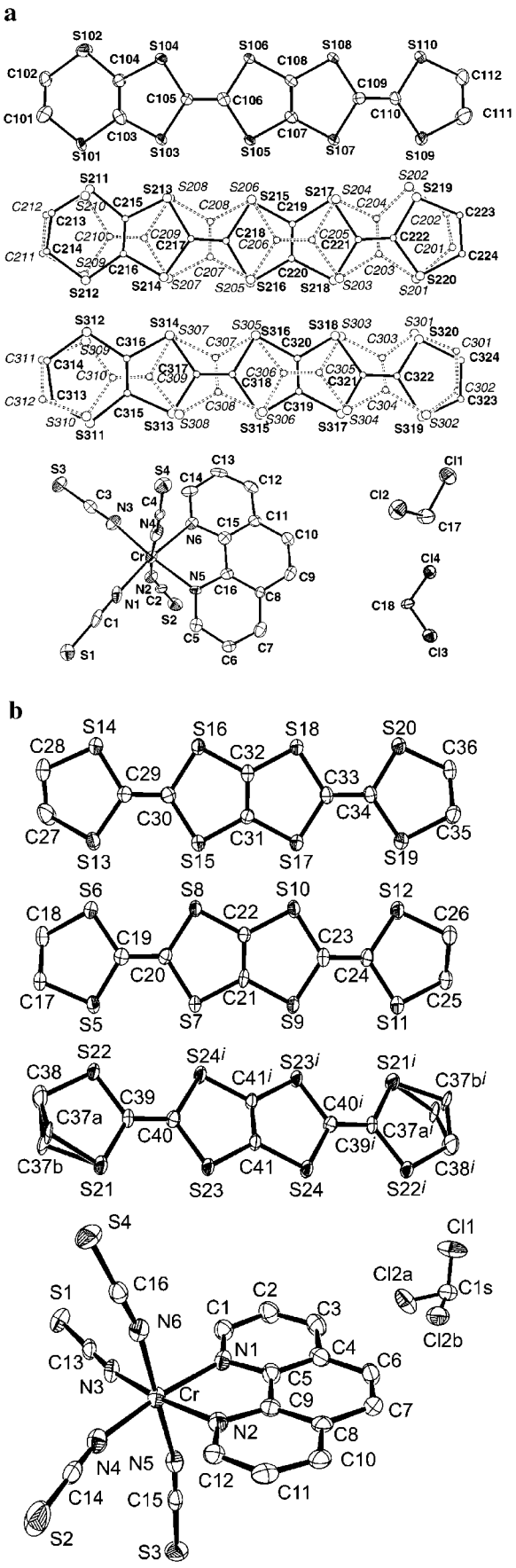

Figure 1. ORTEP diagram with 50% probability level and atom numbering scheme for (a) compound **1**, showing from top to bottom molecule **A** and the disordered molecules **B**, **B′** and **C**, **C′**, and (b) compound **2**.

(20) Murata, K.; Yoshino, H.; Yadav, H. O.; Honda, Y.; Shirakawa, N. *Rev. Sci. Instrum.* **1997**, *68*, 2490.

Table 1. Crystal Data and Structure Refinement for **1** and **2**

	1	**2**
empirical formula	$C_{54}H_{36}Cl_4CrN_6S_{34}$	$C_{42}H_{28}Cl_2CrN_6S_{24}$
fw	2052.73	1509.04
T, K	100	120
cryst syst	monoclinic	monoclinic
space group	$P2_1/a$	$P2_1/a$
a, Å	25.0752(5)	23.8275(4)
b, Å	10.6732(3)	9.1015(2)
c, Å	28.1601(6)	27.0420(1)
β, deg	95.195(2)	99.9297(8)
V, Å^3	7505.6(3)	5776.6(2)
Z	4	4
d_{calcd}, g·cm^{-3}	1.817	1.735
diffractometer	Nonius Kappa CCD	
λ, Mo Kα, Å	0.71073	
θ range, deg	1.72/28.47.	1.53/27.48.
hkl range	−32,27/−13,8/±35	±30, ±11, ±35
reflns collected	21736//939	22157
unique reflns	6741	12961
restraints	502	2
refined params	939	698
$I \geq n\sigma(I)$	6741 [$n = 3$]	12961 [$n = 2$]
R_{int}	0.0513	0.0558
R(F)[a], wR(F)[b,c]	0.0585[a], 0.064[b]	0.0530[a], 0.1196[c]
GOF	1.203	0.992
R min/max, e$^-$·Å^{-3}	−1.09/0.93	−1.297/1.444

[a] $R = \sum||F_o| - |F_c||/\sum|F_o|$. [b] $wR = \{\sum[w(F_o - F_c)^2]/\sum[w(F_o)^2]\}^{1/2}$. [c] $wR = \{\sum[w(F_o^2 - F_c^2)^2]/\sum[w(F_o^2)^2]\}^{1/2}$.

throline) are 1.987(9) and 2.077(7) Å, respectively, which are comparable with those observed for this anion.[13] The Cr−N−CS angles range from 158.8(7)° to 175.4(7)°, the NCS ligands being linear with a mean value of 178.8(8)° for N−C−S angles. The crystal packing (Figure 2a) consists of alternating layers of organic and inorganic units. The structure of the organic layer (Figure 2b) is reminiscent of the well-known κ-type structure in the BEDT-TTF series.[1] There are two different dimers, one noncentrosymmetric dimer formed by the **A** and **B** molecules and a second centrosymmetric dimer formed by the **C** molecule and its symmetrically related one. The shortest S···S contacts (see Table 2 and Figure 2b) between donors (≤3.60 Å = twice of the van der Waals radius for sulfur atom) are established between adjacent dimers as usually observed in this kind of two-dimensional compound. In the inorganic layer, the anion complexes are disposed in such a way that all their NCS ligands are oriented toward the organic layer yielding several $S_{anion}\cdots S_{donor}$ contacts between the anionic and cationic parts (see Table 2 and Figure 2a). Moreover, anion−anion interactions are present in the form of π-stacking between nearest neighbor phenanthroline ligands with interplanar separations of 3.51 Å.

κ_{21}-(BDH-TTP)$_5$[Cr(phen)(NCS)$_4$]$_2$·2CH$_2$Cl$_2$ (2). The geometrical parameters of the $[Cr(phen)(NCS)_4]^-$ anion are close to those observed in compound **1** with mean values for Cr−N (NCS) distances and Cr−N (phenanthroline) equal to 1.988(5) and 2.082(4) Å, respectively. The Cr−N−CS angles range from 162.5(4)° to 170.0(4)°; the NCS ligands are linear with a mean value of 179.1(6)° for N−C−S angles. The crystal packing (Figure 3a) consists of alternating layers of organic and inorganic units. The organic layer (Figure 3b) contains noncentrosymmetric dimers **A** and **B** and monomers **C**, in which each monomer is surrounded by six

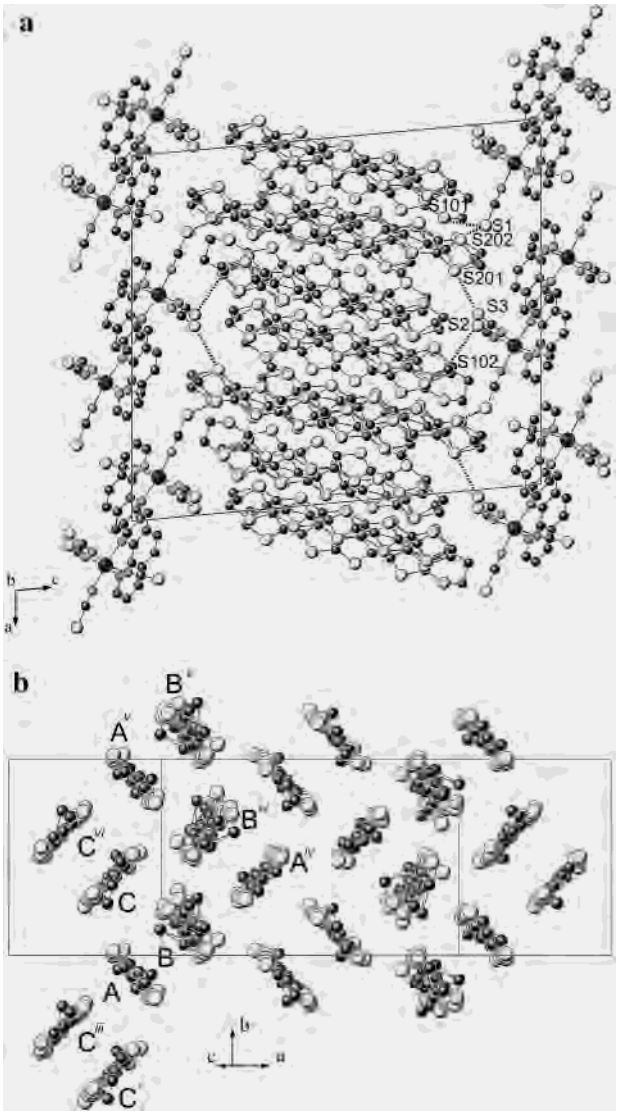

Figure 2. (a) Projection of the crystal structure of **1** in the *ac* plane, showing the layered structure and the π-overlap between the phenanthroline ligands, dashed lines indicate S···S contacts between the organic and inorganic units. (b) Projection of the organic layer in the *ab* plane.

dimers. All intradimer S···S contacts are greater than the sum of the van der Waals radii, while short S···S contacts (≤3.60 Å) are observed between adjacent dimers (see Table 2 and Figure 3b). The S···S contacts between the **C** molecule and the dimer are greater than 3.60 Å indicating that this molecule is isolated. The structure of the organic layer (Figure 3b) resembles the κ-type, but it contains orthogonal dimers and monomers, and then, we called it κ_{21}-type. In our knowledge, only two types of compounds containing dimers and monomers are known, but with different relative arrangements. In one series, namely (BEDT-TTF)$_4$[(A)Fe(C$_2$O$_4$)$_3$]·C$_6$H$_5$CN (A = K, NH$_4$),[21] each centrosymmetric dimer has six neighboring monomers, and in (BEDT-TTF)$_5$[Cr$_2$(C$_2$O$_4$)(NCS)$_8$],[22] the second example reported so far, each monomer is surrounded by four centrosymmetric

(21) Kurmoo, M.; Graham, A. W.; Day, P.; Coles, S. J.; Hursthouse, M. B.; Caulfield, J. L.; Singleton, J.; Pratt, F. L.; Hayes, W.; Ducasse, L.; Guionneau, P. *J. Am. Chem. Soc.* **1995**, *117*, 12209.

Table 2. Intermolecular S···S Contacts (Å) for **1** and **2**

	Compound **1**		
S1···S202[a]	3.521(4)	S1···S101	3.562(3)
S2···S102	3.465(4)	S3···S201[b]	3.518(5)
S101···S301[a]	3.234(6)	S109···S218[c]	3.447(12)
S201···S312[c]	3.263(7)	S209···S217[c]	3.326(12)
S208···S305	3.555(8)	S206···S104	3.585(4)
S212···S217[c]	3.179(17)	S211···S307	3.320(13)
S212···S301[c]	3.407(15)	S218···S109[d]	3.447(12)
S301···S101[e]	3.234(6)	S307···S211	3.320(13)
S301···S209[d]	3.333(8)	S304···S314[f]	3.52(1)
S312···S201[d]	3.263(7)	S311···S110	3.368(7)
S320···S101[e]	3.380(6)	S314···S211	3.472(13)
S314···S304[f]	3.52(1)		
	Compound **2**		
S1···S14[g]	3.590(3)	S5···S24	3.578(2)
S7···S23	3.533(2)	S7···S15[h]	3.510(2)
S8···S24[g]	3.588(2)	S8···S23[g]	3.586(2)
S20···S15[i]	3.523(2)	S16···S17[i]	3.554(2)
S24···S18[a]	3.592(2)		

[a] $x, -1 + y, z$. [b] $x - 1/2, -y - 1/2, z$. [c] $1/2 - x, y - 1/2, 1 - z$. [d] $1/2 - x, y + 1/2, 1 - z$. [e] $x, 1 + y, z$. [f] $-x, 1 - y, 1 - z$. [g] $3/2 - x, y - 1/2, 1 - z$. [h] $1 - x, 1 - y, 1 - z$. [i] $3/2 - x, 1/2 + y, 1 - z$.

dimers. For compound **2**, the comparison of the bond lengths of the donor molecules (Table 3) shows the possibility of charge disproportionation among the donor molecules. The bond length of the central C═C bond in the TTP moiety (bond *a*) is longer for molecule **B** (1.360(7) Å) than for molecules **A** (1.340(7) Å) and **C** (1.343(9) Å). Moreover, the bond length between the TTP moiety and 1,3-dithiolane ring (bond *d*) is slightly shorter for molecule **A** (1.352(7) Å) than for molecules **B** and **C** (1.362(7) and 1.361(7) Å). Therefore, the oxidation degree of the donor molecules is suggested to be in the order **B** > **C** > **A**. As in compound **1**, in the inorganic layer, the anion complexes show a π-stacking between nearest neighbor phenanthroline ligands with interplanar separations of 3.51 Å. The NCS ligands are oriented toward the organic layer yielding several $S_{anion}\cdots S_{donor}$ contacts between the anionic and cationic parts (see Table 2 and Figure 3a).

Electric Conductivity. Figure 4a shows the temperature dependence of the resistivity for compound **1**. As the samples are fragile in general, raw observed data generally show accidental leaps, which are already corrected in the figure. This salt has high conductivity at room temperature (σ_{RT} = 100 S·cm^{-1}) and shows metallic behavior down to T_{min} = 30−50 K depending on the samples. Judging from the sample dependency of T_{min} and nonactivation type behavior of the resistivity below T_{min}, the increase in resistivity in the low temperature regime can be ascribed to the localization caused by the defects and/or impurities within the samples. In other words, it is suggested that the metallic conduction intrinsically perseveres even below T_{min}.

Figure 4b shows the temperature and pressure dependences of the resistivity for compound **2**. The electrical conductivity and activation energy at room temperature and 0 kbar are estimated to $\sigma_{RT} = 2.92$ S·cm^{-1} and $E_A = 46$ meV. As shown in this figure, weak metallic behavior could be observed at 10 and 15 kbar, respectively [metallic above ca. 150 K at 10 kbar, metallic above ca. 170 K at 15 kbar]. One of the possible explanations for the semiconducting behavior in the ambient pressure is the charge separation between the donor molecules as mentioned previously. By applying the pressure, on the other hand, intermolecular overlap between the donor molecules is thought to be increased. This will diminish the charge separation among the donor molecules and realize the weak metallic behavior under the pressure.

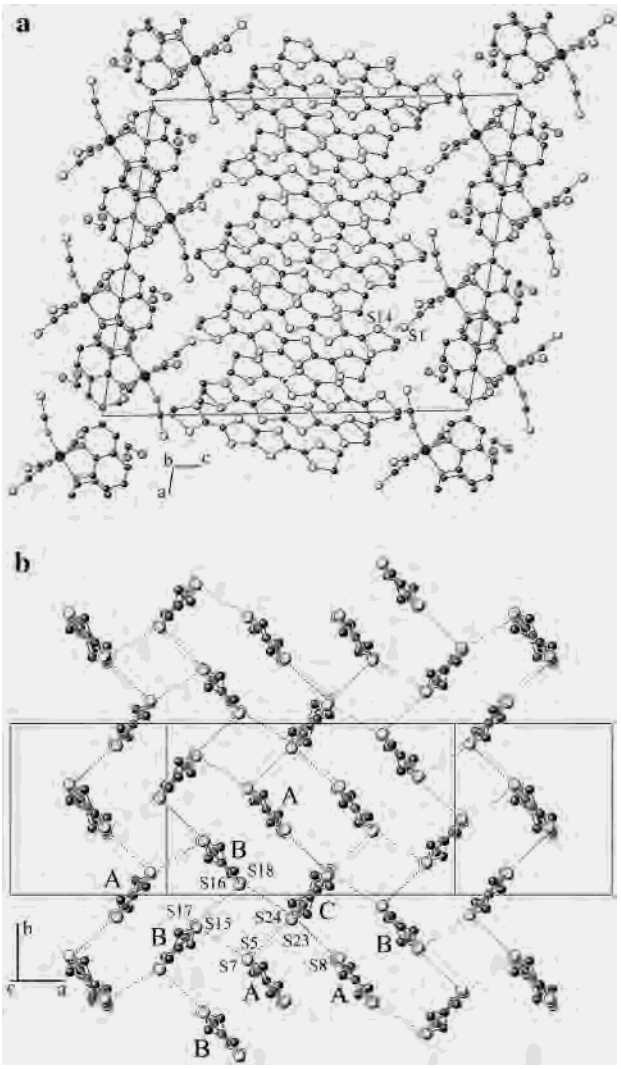

Figure 3. (a) Projection of the crystal structure of **2** in the *ac* plane, showing the layered structure and the π-overlap between the phenanthroline ligands. Dashed lines indicate S···S contacts between the organic and inorganic units. (b) Projection of the organic layer in the *ab* plane; dashed lines indicate the intermolecular S···S contacts ≤3.60 Å (see Table 2).

Table 3. Mean Bond Length Values in the Central BDH-TTP Core for the Three Independent Molecules **A**, **B**, and **C**, in Compound **2**

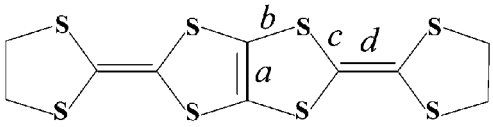

	a	*b*	*c*	*d*
A	1.340(7)	1.740(5)	1.766(5)	1.352(7)
B	1.360(7)	1.733(5)	1.763(5)	1.362(7)
C	1.343(9)	1.741(5)	1.772(5)	1.361(7)

(22) Triki, S.; Bérézovski, F.; Sala Pala, J.; Gomez-García, C. J.; Coronado, E.; Costuas, K.; Halet, J. F. *Inorg. Chem.* **2001**, *40*, 5127.

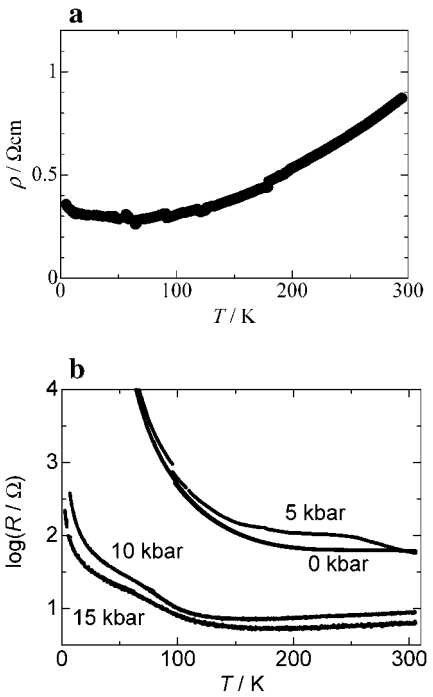

Figure 4. (a) Temperature dependence of the electrical resistivity of compound **1**. The raw experimental data for compound **1** show discontinuous leaps, which are due to the micro cracks and thus corrected. (b) Temperature and pressure dependences of the electrical resistivity of **2**.

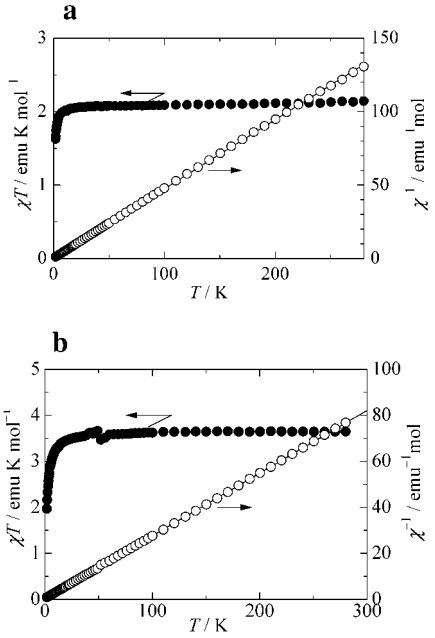

Figure 5. (a) Temperature dependence of χT (●) and χ^{-1} (○) for compound **1**, where χ is the molar paramagnetic susceptibility, with an applied field of 1 T. The solid line is the Curie−Weiss law ($C = 2.125$ emu K mol^{-1}, $\Theta = -0.87$ K). (b) Temperature dependence of χT (●) and χ^{-1} (○) for compound **2**, where χ is the molar paramagnetic susceptibility, with an applied field of 1 T (the peak in the χT curve around 50 K comes from oxygen contamination in the sample chamber of the magnetometer). The solid line is the Curie−Weiss law ($C = 3.667$ emu K mol^{-1}, $\Theta = -1.27$ K).

Magnetic Susceptibility. Figure 5a,b presents the temperature dependence of χT and χ^{-1} for compounds **1** and **2**, where χ is the molar paramagnetic susceptibility after the subtraction of the Pascal core diamagnetic contribution (-1.56×10^{-3} emu·mol^{-1} for **1** and -9.7×10^{-4} emu·mol^{-1} for **2**).

For compound **1**, the susceptibility obeys the Curie−Weiss law with the Curie constant $C = 2.125$ emu·K·mol^{-1} and Weiss temperature $\Theta = -0.87$ K. The deviation of the Curie constant from the spin-only value of Cr^{3+} species (1.875 emu·K·mol^{-1}) can be owed to the weighing error of the small amount of the sample (0.67 mg). The small magnitude of the Weiss temperature shows that little exchange interaction is present between the magnetic counteranions, which is also verified by the magnetization curve measured at 2 K which is fitted with the Brillouin curve for $S = {}^3/_2$.

The susceptibility of compound **2** also shows the Curie−Weiss behavior, with the Curie constant $C = 3.667$ emu·K·mol^{-1} and Weiss temperature $\Theta = -1.27$ K. The Curie constant is close to twice the spin-only value of Cr^{3+} species (1.875 emu·K·mol^{-1}), which indicates that one formula unit contains two counteranions. Although the absolute value of the Weiss temperature is larger than that of **1**, the antiferromagnetic exchange interaction between the magnetic anions is not strong enough to induce a magnetic phase transition above $T = 1.8$ K.

The reason for the small exchange interaction between the anions for both salts is explained as follows. As described previously, the thiocyanate ligands of the anions are oriented toward the organic layer yielding $S_{anion}\cdots S_{donor}$ contacts between the anionic and cationic parts for both salts. However, these contacts do not effectively work for mediating magnetic interaction. For compound **1**, the thiocyanate ligands are connected to the ethylenedithio groups, which contribute little to the HOMO of the donor molecules. Therefore, the magnitude of the π−d interaction for this compound is a small one. For compound **2**, on the other side, the donor sulfur atom that participates in $S_{anion}\cdots S_{donor}$ contact belongs to the 1,3-dithiolane ring, which sufficiently contributes to the HOMO of the donor. However, the nearest path between the anions though the π-electron system is described as anion$\cdots$(donor)$_2\cdots$(donor)$_2\cdots$anion, where (donor)$_2$ denotes a donor dimer, and thus, the magnetic interaction through this path is weak. Moreover, despite the close interplanar separations between nearest neighbor phenanthroline ligands (3.51 Å for both compounds), overlaps between these ligands are, in fact, poor as shown in Figure 6a,b. Therefore, the anion complexes for both compounds are magnetically isolated, which leads to the small magnitude of the Weiss temperatures.

Infrared Spectroscopy. Figure 7 shows the room-temperature reflectance spectra of κ-(EDDH-TTP)$_3$[Cr(phen)(NCS)$_4$]·2CH$_2$Cl$_2$ (**1**) and κ_{21}-(BDH-TTP)$_5$[Cr(phen)(NCS)$_4$]$_2$·2CH$_2$Cl$_2$ (**2**) single crystals, for two perpendicular orientations of the electrical vector of the polarized light, corresponding to the maximum (E_{max}) and minimum (E_{min}) of reflected energy. As can be seen from Figure 7, spectra for each compound are similar in shape. This indicates that the electronic structure is almost isotropic in the *ab* plane for both compounds. Moreover, the reflectance spectra of **2**

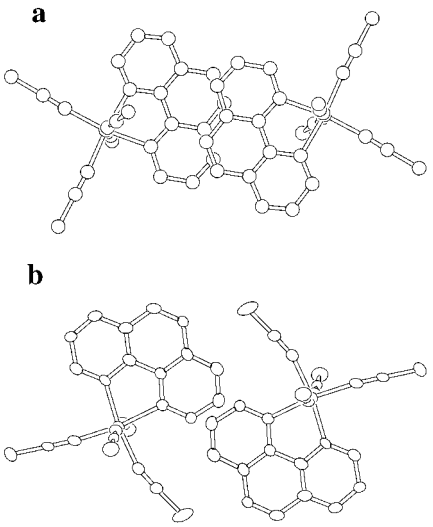

Figure 6. ORTEP drawings of the two neighboring counteranions for compounds (a) **1** and (b) **2**, viewed along the normal planes of the phenanthroline ligands.

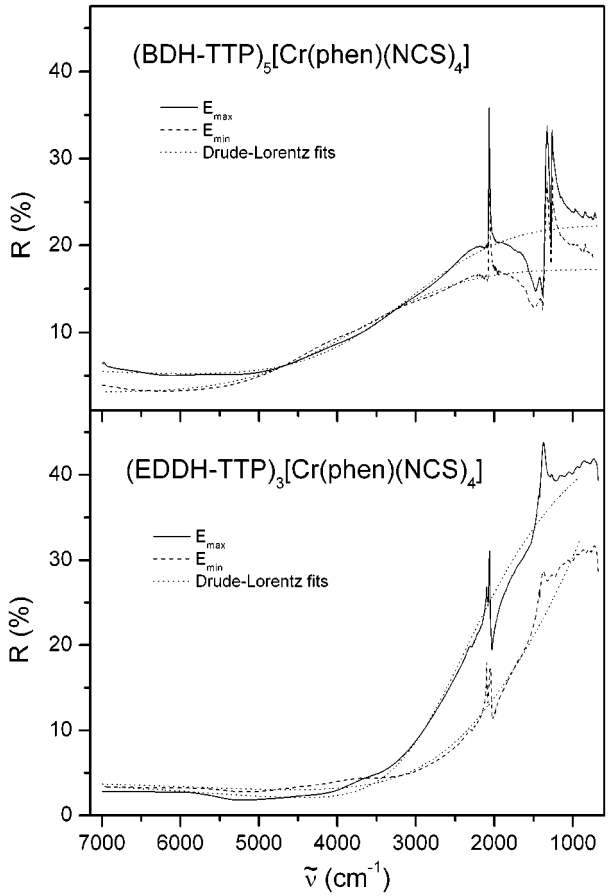

Figure 7. Polarized reflectance spectra of **1** and **2** crystals at room temperature for two perpendicular orientations of the electrical vector of the polarized light, corresponding to the maximum (E_{max}) and minimum (E_{min}) of reflected energy, respectively. Dotted lines show the Drude−Lorentz fits.

exhibit semiconductor-like behavior for both polarizations, while the spectra of **1** resemble spectra of metallic-like materials.

At low frequency, the reflectance and absorption spectra show vibrational features being mostly the consequence of interactions between the charge-transfer transition and the

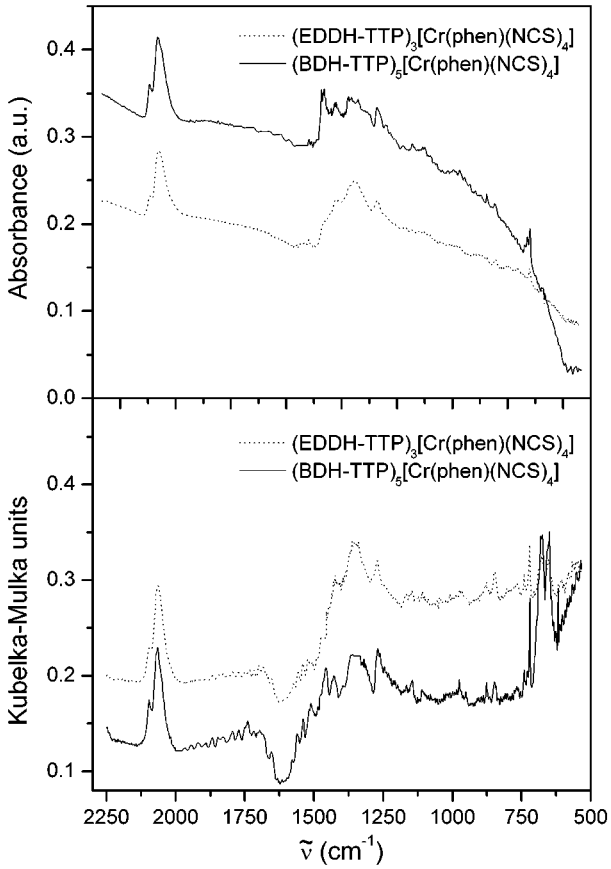

Figure 8. Absorption spectra (upper panel) and diffusion spectra (bottom panel) of **1** and **2** powdered crystals dispersed in KBr.

phonon modes of the BDH-TTP or EDDH-TTP molecule (Figures 7 and 8). The origin of the peaks located near 1260 and 1350 cm^{-1} is due to the coupling of the conduction electrons to intramolecular C═C vibrations of BDH-TTP or EDDH-TTP species, that is, e-mv (electron-molecular vibration) coupling.[23−25] The presence of such bands is a characteristic feature of the IR spectra of BEDT-TTF and TMTTF compounds.[26,27] For our interpretation, we have taken into account the results for BEDT-TTF and TMTTF salts. We attributed the vibrational bands at about 877 and 847 cm^{-1} observed in both polarizations to C—S bond stretching of BDH-TTP or EDDH-TTP molecule and the narrow, intense feature at around 2060 cm^{-1} to the stretching vibration of NCS group of the anion.

To analyze the electronic dispersion, we made least-squares fits to the experimental data of the reflectance calculated from a Drude−Lorentz dielectric function of the form

$$\epsilon(\omega) = \epsilon_\infty + \frac{{\omega_p}^2}{{\omega_0}^2 - \omega^2 - i\omega\Gamma}$$

where ω_0 is the center frequency (energy gap), ω_p is the

(23) Rice, M. J. *Phys. Rev. Lett.* **1976**, *37*, 36.
(24) Lipari, N. O.; Duke, C. B.; Bozio, R.; Girlando, A.; Pecile, C.; Padova, A. *Chem. Phys. Lett.* **1976**, *44*, 236.
(25) Duke, C. B. *Ann. N. Y. Acad. Sci.* **1978**, *313*, 166.
(26) Bozio, R.; Meneghetti, M.; Pecile, C. *J. Chem. Phys.* **1982**, *76*, 5785.
(27) Meneghetti, M.; Bozio, R.; Pecile, C. *J. Phys. (Paris)* **1986**, *47*, 1377.

Table 4. Transport Parameters Obtained from the Analysis of the Reflectance Spectra by the Drude−Lorentz Model

	polarization	ϵ_∞	ω_p (cm^{-1})	Γ (cm^{-1})	ω_0 (cm^{-1})
$(BDH\text{-}TTP)_5[Cr(phen)(NCS)_4]$	E_{max}	3.1	5720	3850	2640
	E_{min}	2.5	5850	4380	3210
	E_{max}	2.5	4940	2440	820
$(EDDH\text{-}TTP)_3[Cr(phen)(NCS)_4]$	E_{min}	2.5	4610	3370	350

plasma frequency, Γ is the relaxation rate, and ϵ_∞ represents all higher frequency contributions to the dielectric function. The fits were made to the reflectance between 1800 and 7000 cm^{-1}. Below 1800 cm^{-1}, the short range of both electron−phonon and electron−electron interactions yields distinct deviations from the simple Drude−Lorentz behavior. Nevertheless, it is assumed that the plasmon frequency is insensitive to the detailed nature of these interactions.[28] The derived Drude−Lorentz parameters are listed in Table 4, and the quality of the fits is shown in Figure 7.

Band Structure Calculations. Electronic band structures for **1** were calculated with the tight-binding method using the extended Hückel Hamiltonian.[29] The energy dispersion curves and the Fermi surfaces calculated are shown in Figure 9.

Although compound **1** has the κ-type structure, the shape of its Fermi surface is different from the shape characteristic for the typical κ-type salt such as κ-$(BEDT\text{-}TTF)_2[CuN(CN)_2Br]$.[1] Namely, the κ-type Fermi surface consists of one-dimensional orbit and two-dimensional orbit, whereas the Fermi surface of compound **1** is made of small orbits, a hole pocket at the Γ point, and two electron pockets around (0, $\pm 0.35b^*$). This is due to the differences in the number of molecules within the unit cell (κ-type, 4; compound **1**, 12) and the filling ratio (κ-type, 3/4; compound **1**, 5/6). In any case, this compound has the quasi-two-dimensional Fermi surfaces, which is the origin of the metallic conduction down to low temperatures.

Conclusion

Two charge-transfer salts composed of new types of organic π-electron donors, EDDH-TTP and BDH-TTP, and the paramagnetic $[Cr^{III}(phen)(NCS)_4]^-$ anion were investigated. The EDDH-TTP salt has the κ-type structure donor alignment, resulting in the metallic electric conduction down to low temperatures, which is consistent with the result of band structure calculation. The BDH-TTP salt has the κ_{21}-type structure composed of donor dimers and monomers. This salt shows semiconductive behavior due to either Peierls distortion or charge disproportionation. For both compounds, infrared data are in good agreement with electrical conductivity measurements. The magnetic susceptibility results show Curie−Weiss behavior with small magnetic interaction between the paramagnetic anions. The weakness of the exchange interaction is explained by the poor overlap between the anions and donors through S···S contacts and also between the anions through the phenanthroline ligands.

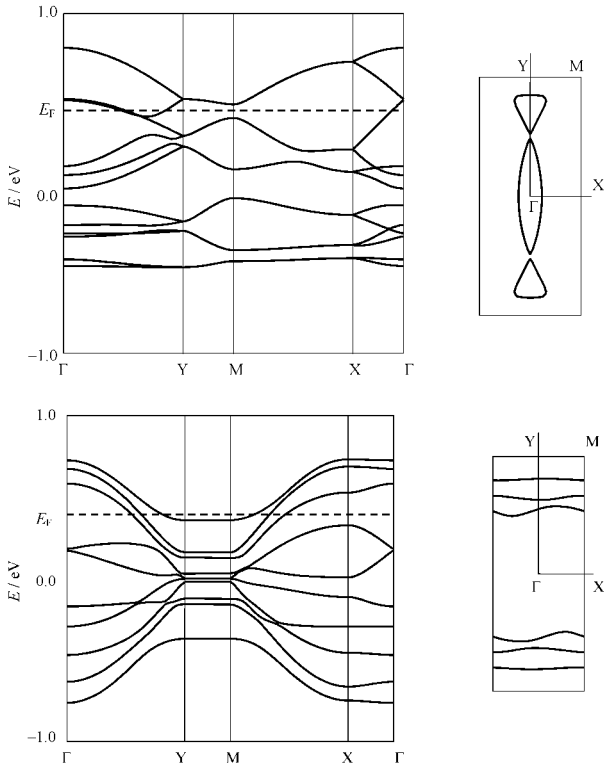

Figure 9. Energy dispersion curves (left) and Fermi surface within the first Brillouin zone (right) for compound **1**. Dashed line in the energy dispersion curve denotes the Fermi level.

Acknowledgment. Financial support from CNRS and CNRS-JSPS exchange program 9473 and Polonium exchange program 03273NK is acknowledged. F.S. thanks the Algerian and French Ministries of Education for a Ph.D. fellowship.

Supporting Information Available: X-ray crystallographic file, in CIF format. This material is available free of charge via the Internet at http://pubs.acs.org.

IC0255961

(28) Jacobsen, C. S. *J. Phys. C: Solid State Phys.* **1986**, *19*, 5643.
(29) Mori, T.; Kobayashi, A.; Sasaki, Y.; Kobayashi, H.; Saito, G.; Inokuchi, H. *Bull. Chem. Soc. Jpn.* **1984**, *57*, 627.